J Mater Sci (2011) 46:5245–5251
DOI 10.1007/s10853-011-5462-3

# Characterization of deformation mechanisms during low cycle fatigue of a single crystal nickel-based superalloy

**H. U. Hong · B. G. Choi · I. S. Kim · Y. S. Yoo · C. Y. Jo**

Received: 30 January 2011 / Accepted: 9 March 2011 / Published online: 16 March 2011


**Abstract** The deformation and fracture mechanisms of a single crystal nickel-based superalloy CMSX-4 have been investigated during low cycle fatigue (LCF) tests at temperatures of 750, 850, and 950 °C under strain-controlled $R = 0$. It was found that LCF lives at 750 and 850 °C were similar and longer than those at 950 °C. The specimens tested at 750 and 850 °C showed fatigue crack initiation at internal pores, and their failure occurred by cracking at persistent {111} slip bands. On the other hand, at 950 °C the crack initiated at the oxide-layered surface and propagated along <100> $\gamma$ channel until fracture. At the two lower temperatures, $a/2$<110> dislocations with low density was rarely present within $\gamma$ channels, and $a/3$<211> partial dislocations were occasionally seen to shear $\gamma'$ leaving superlattice stacking faults behind. At 950 °C, homogeneous deformation was produced by perfect dislocation movements of cross-slip and climb in the $\gamma$ channel and a limited $\gamma'$ shearing by superdislocation was observed. At total strain range lower than 0.6%, well-developed polygonal dislocation network formed at rafted $\gamma'$ interface. Comparison of dislocation structures revealed that load-controlled LCF tests lead to more severe deformation to specimens than strain-controlled tests.

## Introduction

Turbine blades and vanes in gas turbines and aeroengines are subjected to very high temperatures and mechanical loads. Recently, these hot section components are made of single crystal nickel-based superalloys in order to withstand the critical loadings resulted from the complex combination of high thermal and high mechanical loadings. Accordingly, the creep properties in the single crystal nickel-based superalloys have been studied in great detail. However, since the hot section components are also subjected to cyclic thermal stresses resulting from start-up and shut-down, low cycle fatigue (LCF) at high temperatures has been an area of ever-growing interest for the past several decades [1–8]. Most studies dealing with the LCF of nickel-based superalloys focused on the macroscopic properties under a strain ratio of $R = -1$. In order to simulate more closely the operating condition of gas turbines, repeated LCF tests with $R = 0$ have been recently investigated [4–8].

There are relatively few articles investigating the microstructural degradation of current second generation single crystal superalloy CMSX-4 during LCF although the prediction of the deformation mechanisms is an essential part of the safe designing against fatigue. MacLachlan and Knowles [6] studied high cycle fatigue (HCF) and LCF of CMSX-4 at the temperatures of 750, 850, and 950 °C under load-controlled $R = 0$. Tests at a single stress level at each temperature were carried out. They reported that at low temperatures and high frequencies, crystallographic crack growth occurred rapidly along persistent slip bands (PSBs). As temperature increased or frequency reduced, deformation became similar to creep, displaying dislocation networks spread homogeneously through the $\gamma$ channel. The failure under these conditions occurred by planar stage II crack growth. However, the single stress test did not allow to represent the whole deformation behaviors and to compare with other data. Whan and Rae [7] considered the deformation microstructures of CMSX-4 under $R = 0$ LCF

H. U. Hong (✉) · B. G. Choi · I. S. Kim · Y. S. Yoo · C. Y. Jo
High Temperature Materials Research Group, Korea Institute of Materials Science, 797 Changwondaero, Changwon, Gyeongnam 641-831, South Korea
e-mail: hnk@kims.re.kr

tests with stresses both above and below yield stress. They observed that cyclic deformation above yield stress at 750 °C developed extensive penetration of the $\gamma'$ by dislocation dipoles and by partial dislocations trailing stacking faults (SFs). Charles et al. [8] gave a detailed observation on the above dipoles, and identified them as dislocation loops in the $\gamma'$ trailing either antiphase boundary (APB) or SFs. The microstructures of test cycled at stresses above yield stress at 950 °C showed no evidence of rafting but dislocation pairs shearing the $\gamma'$ precipitates [7, 8]. All the articles mentioned above concerned the deformation behaviors of CMSX-4 during load-controlled LCF tests. Little literature has been found related with the deformation behaviors of CMSX-4 during strain-controlled LCF even though the strain-based approach to fatigue design has found much appeal to understand more realistic material behaviors [9]. Although Sakaguchi and Okazaki [10] carried out strain-controlled thermo-mechanical fatigue (TMF) and LCF tests of CMSX-4, they focused on the life prediction model rather than on the detailed investigation of deformation mechanisms.

In the present study, the deformation and fracture mechanisms of a single crystal nickel-based superalloy CMSX-4 were investigated during strain-controlled LCF tests at temperatures of 750, 850, and 950 °C. This article also discussed the comparison of deformation microstructures between load-controlled and strain-controlled LCF tests.

## Experimental procedures

The material investigated in the present work is a second generation single crystal superalloy, CMSX-4. The nominal composition is Ni–6.5Cr–9Co–0.6Mo–6W–1.0Ti–6.5Ta–3Re–0.1Hf–5.6Al (in weight percent). All castings were made using master ingots (made by Cannon-Muskegon) from a single heat. Single crystals were cast with rods of 13 mm diameter in a vacuum furnace (ALD model ISP 0.5) by Bridgman method. The cast rods were oriented near [001] direction with a maximum deviation of 9°. For this material, the heat treatments were given as follows: the solution treatment at 1,320 °C for 2 h, and then the two step aging treatments at 1,140 °C for 2 h and at 871 °C for 20 h in vacuum status of $1 \times 10^{-5}$ torr. This heat treatment produced a microstructure consisting of cuboidal ordered $L1_2$-structured $\gamma'$ precipitates embedded coherently in the $\gamma$ matrix of fcc structure, as shown in Fig. 1. As previously reported [11], the volume fraction and the size of cuboidal $\gamma'$ precipitates were 60% and about 400–500 nm, respectively. Figure 1b displays the $\gamma'$ cuboids aligned regularly along crystallographic directions, and very low dislocation density. According to earlier studies [12, 13], the constrained lattice misfit of $\gamma/\gamma'$ interface is negative and in the order of $-10^{-3}$ at room temperature.

LCF specimens were machined from single crystal bars. The cylindrical solid specimens had a gauge length of 16 mm and a diameter of 5 mm. The specimens were mechanically polished before fatigue tests to prevent premature crack initiation at surface-machined scratches. The strain-controlled LCF tests were carried out in air to failure on a servo-hydraulic fatigue machine (Instron 8501) with a capacity of ±100 kN load cell. The LCF tests were conducted at temperatures of 750, 850, and 950 °C under strain ratio of $R = 0$. A trapezoidal waveform with a total strain range ($\Delta\varepsilon_{tot}$) of 0.6–1.2% was imposed consisting of 1 s ramps and a 1 s dwell at maximum and zero strain (1-1-1-1 waveshape). The life of LCF was defined as the number of cycles at which the specimen was broken.

For the observation on the fractured surfaces and deformed microstructures, scanning electron microscopy (SEM) examination was performed on a JEOL JSM-5800 microscope with a tungsten filament operating at 20 keV. To prepare thin foils for transmission electron microscope (TEM) examination, the fatigued specimens were cut perpendicular to the stress axis using a low-speed diamond saw to obtain thin sheets. Three-millimeter-diameter disks were punched out from the thin sheets, and electropolished to

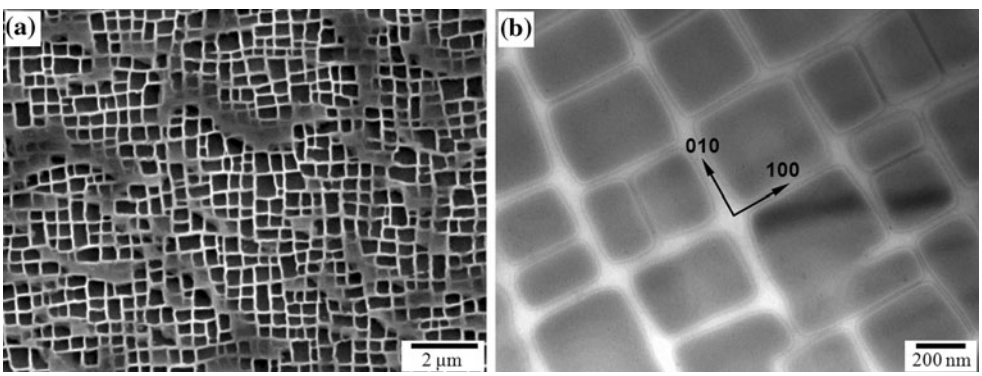


**Fig. 1** Initial microstructure of CMSX-4: **a** SEM and **b** TEM micrographs

perforation with an 80% methanol and 20% perchloric acid electrolyte at −25 °C and 20 V, using a double-jet electropolisher. The TEM characterization was performed on a field emission type JEOL JEM-2100F operating at 200 keV. Some of the TEM observations have been done with the foils prepared by a focused ion beam (FIB) system to investigate deformed microstructures near fatigue crack tips.

## Results and discussion

### Cyclic stress–strain behavior

Figure 2 shows the typical hysteresis loops at each strain and temperature. The loops are given by those at the first cycle ($N = 1$) and at the mid-life ($N = N_f/2$, where $N_f$ is the number of cycles to failure). With increasing the number of cycles, the loop shifted downwards during LCF cycling regardless of test conditions. The downward shift of hysteresis loop is characteristics of the LCF test with $R = 0$, where the decrease in the maximum tensile stress is frequently observed [10, 11]. The degree of decrease in the maximum tensile stress became larger with increasing temperature even though there was little significant difference in plastic strain range regardless of total strange range and temperature. The decrease in the maximum tensile stress at each temperature results from stress relaxation which occurs during 1 s dwell at maximum strain at each cycle. The stress relaxation at elevated temperatures could be caused by the weakened $\gamma/\gamma'$ coherency (the formation of interfacial dislocations associated with $\gamma/\gamma'$ rafting) and/or plastic deformation by significant dislocation movements in $\gamma/\gamma'$ (climbing, $\gamma'$ shearing, and mechanical twinning) [11, 14]. It should be noted that although the specimens were cycled at the highest strain range, the maximum tensile stresses at mid-life exhibited less than 900 MPa at 750 °C, 850 MPa at 850 °C, and 630 MPa at 950 °C, respectively. These maximum stresses are much lower than those applied to the specimens for load-controlled LCF tests in the previous studies [7, 8], which implies that the deformed microstructures in the present study could be different. In the following section, microstructural evolution will be discussed with a consideration of cyclic stress–strain behaviors.

Figure 2d shows the cyclic stress–strain behavior at each temperature. The cyclic strain hardening behavior appears to be almost similar at all temperatures, and its exponent is about 0.885.

### LCF lives

The relationship between the total strain range and the number of cycles to failure is plotted in Fig. 3. It was found that LCF lives at 750 and 850 °C were similar, however, those at 950 °C were much shorter. This implies that there may be detrimental factors leading to a significant decrease

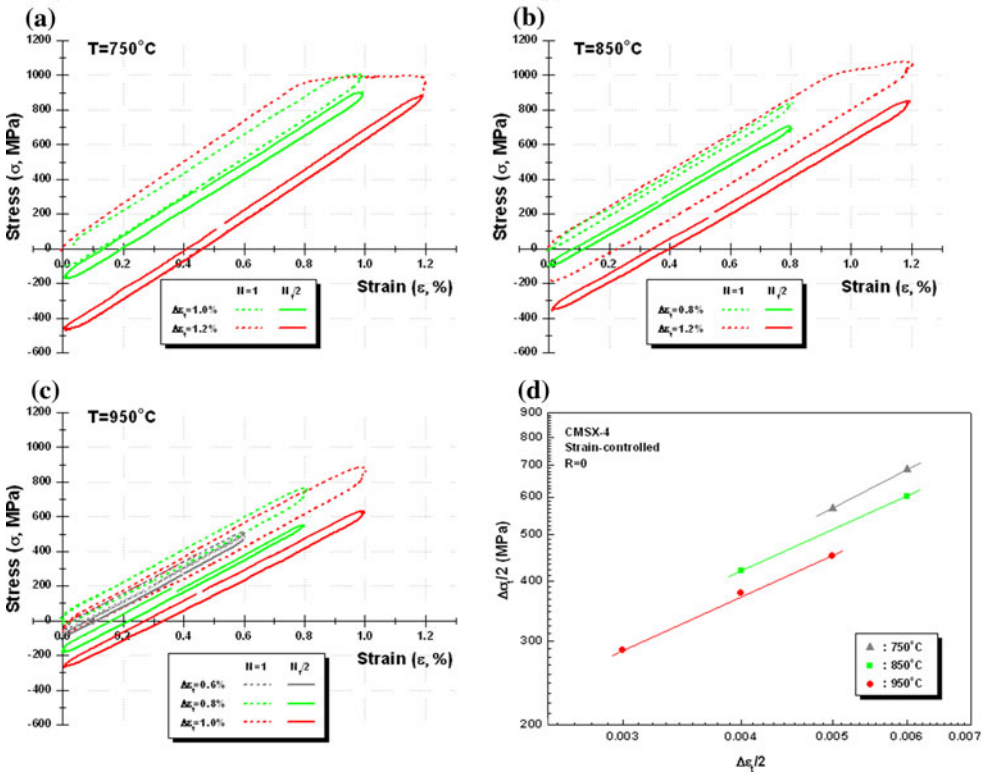


**Fig. 2** Typical hysteresis loops at **a** 750 °C, **b** 850 °C, **c** 950 °C, and **d** cyclic stress–strain behavior

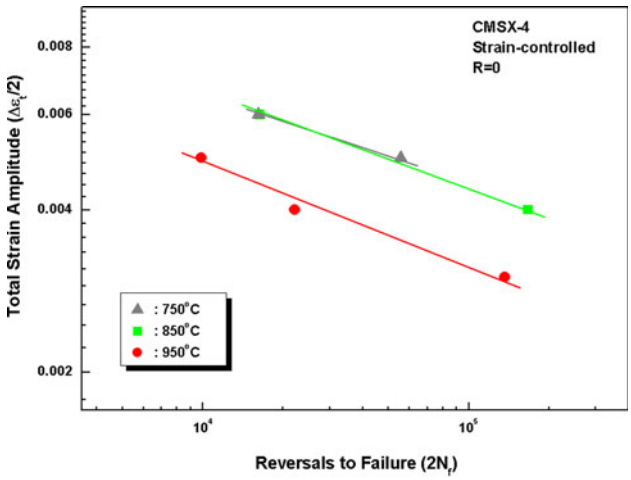


**Fig. 3** LCF lives of CMSX-4 at different temperatures

in fatigue life at 950 °C, and a similar fatigue failure mechanism at the two lower temperatures could be expected. In order to understand the fatigue failure mechanisms, metallographic analysis was employed and the details will be discussed in the following section.

## Deformation and failure mechanisms during LCF cycling

The fractured surfaces and cross-sections after LCF tests are presented in Fig. 4. It is evident that across the temperature range of 850–950 °C, a transition of fatigue failure mode occurred from internal pore-initiated fracture to surface-initiated fracture. At 750 and 850 °C, the crack initiated at a pore below surface, and its planar growth under vacuum left traces of a circular region. After the internal crack grew over a certain size, a large amount of stress field near the crack tip caused the failure by cracking along persistent {111} slip bands. At 950 °C, a change occurred: surface cracks formed at the oxide scale during cycling and propagated into bulk specimen, as shown in Fig. 4g–i. Thus, it can be suggested that when the CMSX-4 is primarily exposed above 950 °C the resistance to surface oxidation is crucial for enhancement of LCF property, while casting process with minimal defects is priority at and below 850 °C.

Figure 5 shows the deformed microstructures at 750 °C under $\Delta\varepsilon_{tot} = 1.0\%$. A very low density of dislocations was inhomogeneously present within $\gamma$ channels. Oriented slip

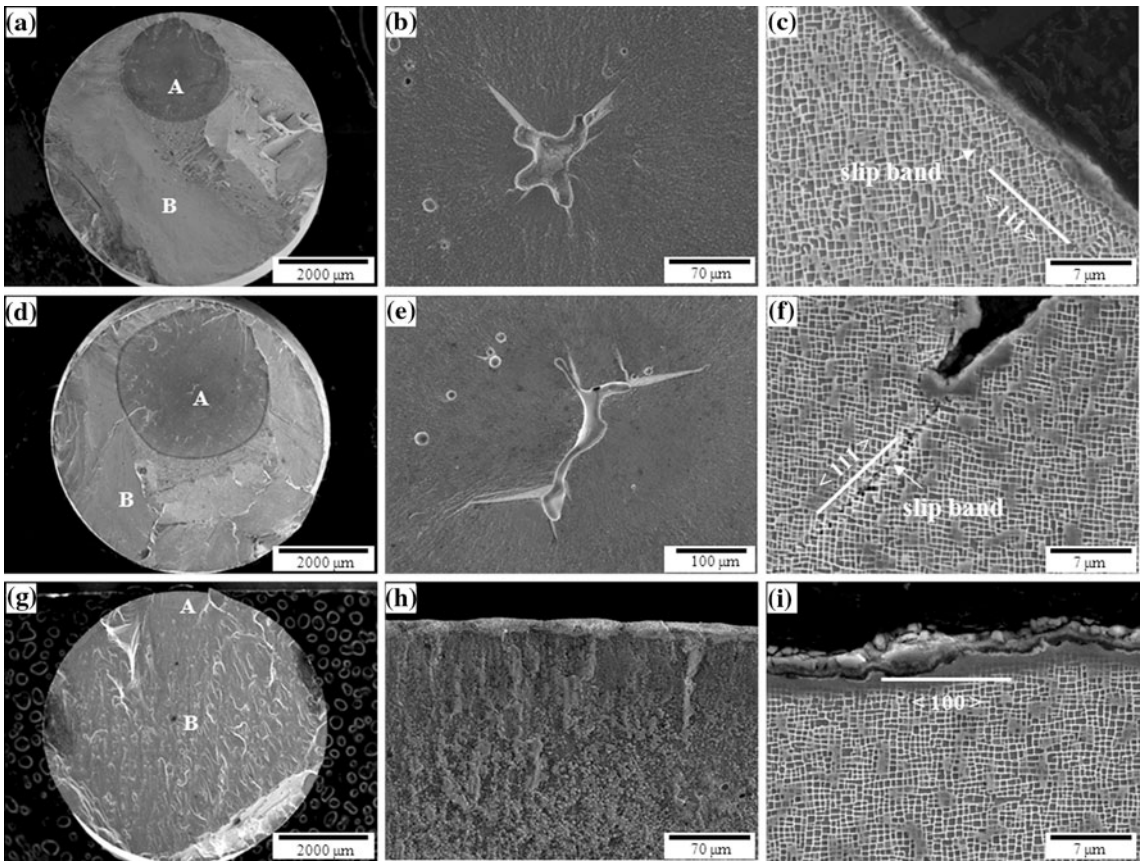


**Fig. 4** SEM images showing fractured surfaces, crack initiation regions, and cross-sections: **a**, **b**, and **c** at 750 °C/1.0%, **d**, **e**, and **f** at 850 °C/0.8%, **g**, **h**, and **i** at 950 °C/1.0%. In fractured surfaces '*A*' corresponds to crack initiation region, and '*B*' corresponds to location examined by cross-sectional observation

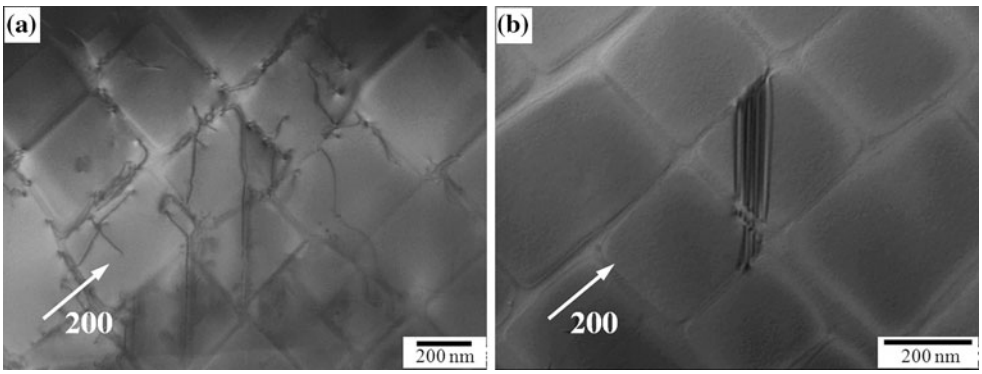


**Fig. 5** Deformed microstructures showing **a** a very low dislocation density in $\gamma$ channels and **b** SFs in the $\gamma'$ phase after LCF test at 750 °C/ $\Delta\varepsilon_{tot} = 1.0\%$

was occasionally observed as a result of primary slip operation with high Schmid factor and identified as $a/2<110>$ matrix dislocation, as shown in Fig. 5a. This dislocation structure is similar to that after HCF interruption test at 2/3 of the full life under condition of 750 °C and 820 MPa [6]. However, no evidence of $\gamma'$ shearing by this oriented slip was observed in the present study. Instead, partial dislocations were sparsely seen to shear $\gamma'$ leaving superlattice SFs behind. Many literature [5, 15–17] have shown that these SFs form by the decomposition of an interfacial $a/2[110]$ matrix dislocation into $a/3[211]$ and $a/6[112]$ at intermediate temperature deformation regime: the $a/3<211>$ partial enters the $\gamma'$ precipitate, creating an SF, while the $a/6<112>$ partial remains in the interface. This deformation behavior is quite different from previous studies [7, 8] describing that deformation above yield stress at 750 °C developed a high dislocation density within $\gamma$ channels, and extensive $\gamma'$ shearing by dislocation loops trailing either APB or SFs.

Figure 6 shows the deformed microstructures at 850 °C under $\Delta\varepsilon_{tot} = 0.8\%$. The dislocation activity was essentially same as that after LCF test at 750 °C. A low density of dislocations within $\gamma$ channels and SFs after $\gamma'$ shearing by the passage of $a/3<211>$ partial dislocations were sporadically seen. However, the dislocation movement became slightly more activated by cross-slip which is necessary for spreading of the dislocations into the narrow $\gamma$ channels, resulting in the highly oriented or bowing dislocation configuration. The recent works [7, 8] reported a more heavily dislocated structures within $\gamma$ channels after load-controlled LCF test at 850 °C than the present study.

No significant difference in deformed microstructures was observed at both 750 and 850 °C except a slight change of dislocation movement within $\gamma$ channels. Additionally, the fatigue failure mechanism was identical at the two temperatures: the crack initiated at an internal pore since surface oxidation was not detrimental enough in the CMSX-4. Thus, a similar LCF life at 750 and 850 °C could be understood. However, it is generally known that the LCF life is normally decreased with increasing temperature [9]. Nevertheless, the similar LCF life could be associated with the combination of similar failure mode and deformation behavior at the two temperatures. It is also accepted that the LCF life becomes longer with increasing ductility of the material [9]. It is interesting that the elongation of CMSX-4 after tensile test was higher at 850 °C (29.7%)

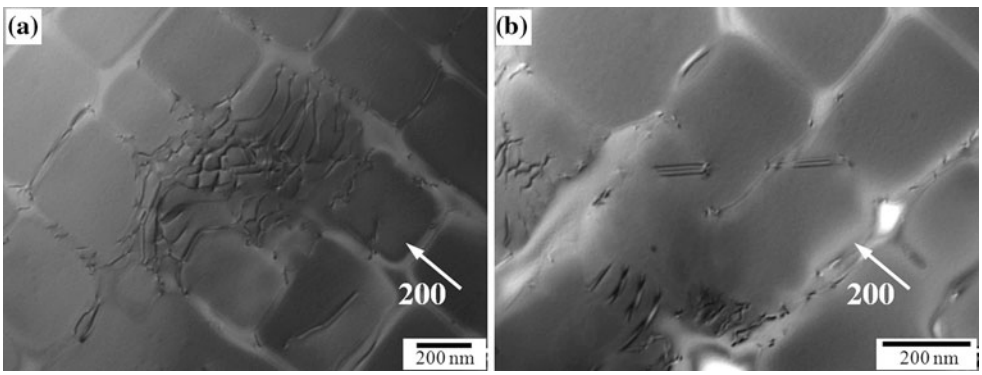


**Fig. 6** Deformed microstructures showing **a** a very low dislocation density in $\gamma$ channels and **b** SFs in the $\gamma'$ phase after LCF test at 850 °C/ $\Delta\varepsilon_{tot} = 0.8\%$

**Table 1** Tensile properties of CMSX-4 at 750, 850, and 950° C

| | Yield strength (MPa) | Tensile strength (MPa) | Elongation (%) |
|---|---|---|---|
| 750 °C | 1,032 | 1,273 | 14.2 |
| 850 °C | 966 | 986 | 29.7 |
| 950 °C | 737 | 905 | 23.9 |

than at 750 °C (14.2%), as shown in Table 1. Therefore, it appears that the higher ductility at 850 °C compensates with the retardation of crack initiation and propagation at internal pore.

At 950 °C, the deformed microstructures were distinguishable depending on whether the raft was developed or not. Figure 7 shows the $\gamma/\gamma'$ microstructures near fractured surfaces. Only at the total strain range of 0.6%, significant $\gamma'$ rafts were observed perpendicular to the stress axis. This result implies that the development of rafts is largely dependent on time rather than applied strain. Whan and Rae [7] also found that the $\gamma'$ rafts were developed at 950 °C under the lower applied stress (480 MPa). Matan et al. [18] studied the kinetics of rafting during creep of CMSX-4. They suggested that $\gamma'$ rafting was independent of the applied stress if a threshold strain of 0.10 ± 0.03% was achieved, and the incubation time should be provided to generate sufficient diffusion and dislocation density to initiate rafting during creep. Thus, it is suggested from the present study that a threshold length of test enabling a considerable rafting to occur may exist in the range between 12 h ($\Delta\varepsilon_{tot} = 0.8\%$) and 76 h ($\Delta\varepsilon_{tot} = 0.6\%$) during LCF with $R = 0$. Figure 8 shows the deformed microstructures at 950 °C under $\Delta\varepsilon_{tot} = 0.6$ and 1.0%. At the total strain range of 1.0% (Fig. 8b), dislocations were more homogeneously spread throughout the $\gamma$ channels compared with Figs. 5 and 6. The superdislocations with {111}<011> slip system were occasionally observed to shear the $\gamma'$ precipitates. At the total strain range of 0.6% where significant rafts occurred, almost all the dislocations were associated with the formation of interfacial network at the rafted $\gamma/\gamma'$ interface and they generated a well-developed polygonal network. Each dislocation line was composed of a few sets of dislocations with Burgers vectors of *a*/2<110>. This dislocation structure is identical to that taken from a crack tip [11], which reflects that LCF tests produce homogeneous deformation throughout a specimen unlike TMF tests. No SFs were seen at any strain range.

Based on the series of observations, the deformation mechanisms of CMSX-4 during strain-controlled LCF with $R = 0$ can be schematically summarized, as shown in Fig. 9.

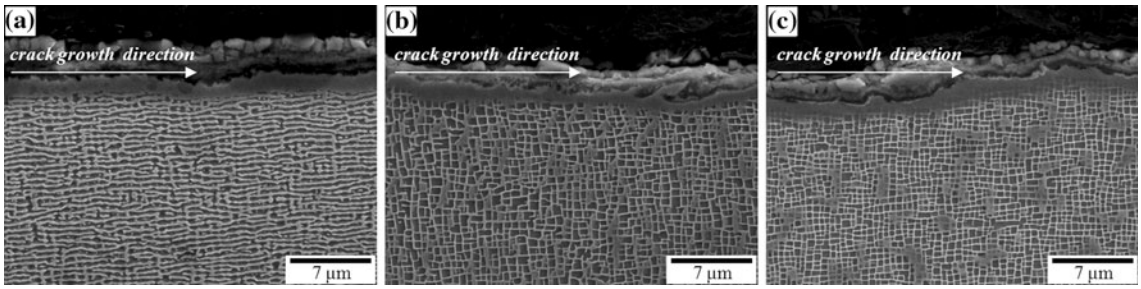


**Fig. 7** SEM images showing $\gamma/\gamma'$ microstructures near fractured surfaces after LCF test at 950 °C: **a** $\Delta\varepsilon_{tot} = 0.6\%$, **b** $\Delta\varepsilon_{tot} = 0.8\%$, and **c** $\Delta\varepsilon_{tot} = 1.0\%$

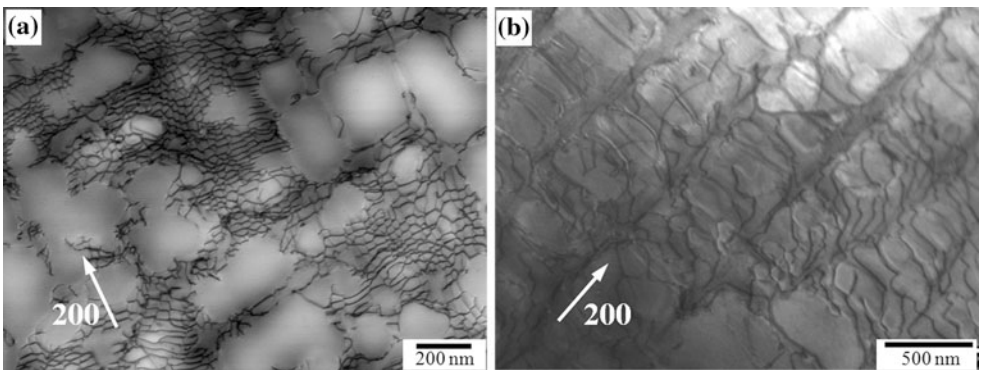


**Fig. 8** Deformed microstructures after LCF test at 950 °C: **a** $\Delta\varepsilon_{tot} = 0.6\%$ and **b** $\Delta\varepsilon_{tot} = 1.0\%$

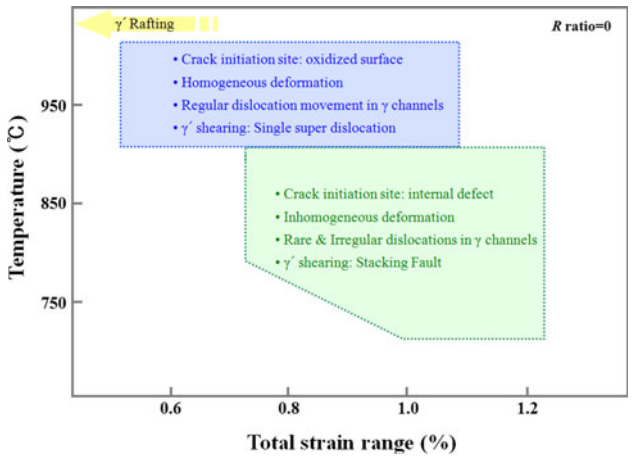


**Fig. 9** Schematic illustration of the deformation mechanisms of CMSX-4 during strain-controlled LCF cycling with $R = 0$

## Conclusions

The deformation and fracture mechanisms of CMSX-4 have been characterized during strain-controlled LCF tests with $R = 0$ at temperatures of 750, 850, and 950 °C. The main conclusions can be drawn as follows:

1. It was found that LCF lives at 750 and 850 °C were similar and longer than those at 950 °C. Across the temperature range of 850–950 °C, a transition of fatigue failure mode occurred from internal pore-initiated fracture to surface-initiated fracture.
2. At 750 and 850 °C, no significant difference in deformed microstructures was observed except a slight change of dislocation movement within $\gamma$ channels: a very low density of dislocations with $a/2<110>$ was inhomogeneously present within $\gamma$ channels, and $a/3<211>$ partial dislocations were occasionally seen to shear $\gamma'$ leaving SFs behind.
3. At 950 °C, homogeneous deformation was produced by perfect dislocation movements of cross-slip and climb in the $\gamma$ channel and a limited $\gamma'$ shearing by superdislocation was observed. At total strain range lower than 0.6%, well-developed polygonal dislocation network formed at rafted $\gamma'$ interface.
4. Comparison of dislocation structures revealed that load-controlled LCF tests lead to more severe deformation to specimens than strain-controlled tests.
5. When the CMSX-4 is primarily exposed at 950 °C the resistance to surface oxidation is crucial for enhancement of LCF property, while casting process with minimal defects is priority at and below 850 °C.

**Acknowledgements** The authors acknowledge the financial support of MKE (Ministry of Knowledge Economy), Account No. UCN248-2865.C, which made this work possible.

## References

1. Anton DL (1984) Acta Metall 32:1669
2. Fleury E, Rémy L (1993) Mater Sci Eng A 167:23
3. Ott M, Mughrabi H (1999) Mater Sci Eng A 272:24
4. Brien V, Décamps B (2001) Mater Sci Eng A 316:18
5. Zhou H, Ro Y, Harada H, Aoki Y, Arai M (2004) Mater Sci Eng A 381:20
6. MacLachlan DW, Knowles DM (2001) Fatigue Fract Engng Mater Struct 24:503
7. Whan CM, Rae CMF (2003) In: Strang A et al (eds) Proceedings of the 6th international Charles Parsons turbine conference (PARSONS 2003). Maney publishing for the institute of materials, minerals and mining, Dublin, Ireland, pp 789–801
8. Charles CM, Drew GA, Bagnall S, Rae CMF (2007) Mater Sci Forum 546–549:1211
9. Suresh S (2001) Fatigue of materials, 2nd edn. Cambridge University Press, Cambridge, UK
10. Sakaguchi M, Okazaki M (2006) JSME Int J 49:345
11. Hong HU, Kang JG, Choi BG, Kim IS, Yoo YS, Jo CY (2010) Int J Fatigue (under review)
12. Völkl R, Glatzel U, Feller-Kniepmeier M (1998) Acta Mater 46:4395
13. Nathal MV, Mackay RA, Garlick RG (1985) Mater Sci Eng 75:195
14. Zhang JX, Ro Y, Zhou H, Harada H (2006) Scripta Mater 54:655
15. Caron P, Khan T, Veyssière (1988) Philos Mag A 57:859
16. Condat M, Décamps B (1987) Scripta Metall 21:607
17. Milligan WW, Antolovich SD (1991) Metall Tans A 22:2309
18. Matan N, Cox DC, Rae CMF, Reed RC (1999) Acta Mater 47:2031